

Magnetic properties of $(\text{Co}_{0.65}\text{Fe}_{0.35})_{1-x}(\text{Ni}_{0.5}\text{Zn}_{0.5}\text{Fe}_2\text{O}_4)_x$ bi-magnetic composite granular films for high frequency application

Guozhi Chai, Dangwei Guo, Xiling Li, Jingyi Zhu, Wenbo Sui and Desheng Xue¹

Key Lab for Magnetism and Magnetic Materials of the Ministry of Education, Lanzhou University, Lanzhou 730000, People's Republic of China

E-mail: xuedsh@lzu.edu.cn

Received 27 April 2009, in final form 19 August 2009

Published 24 September 2009

Online at stacks.iop.org/JPhysD/42/205006

Abstract

A series of $(\text{Co}_{0.65}\text{Fe}_{0.35})_{1-x}(\text{Ni}_{0.5}\text{Zn}_{0.5}\text{Fe}_2\text{O}_4)_x$ bi-magnetic composite granular films with different ferrite atom fraction x are fabricated by magnetron sputtering. Scanning electron micrographs and x-ray diffraction results show that the films consist of bcc $\text{Co}_{0.65}\text{Fe}_{0.35}$ particles, uniformly with particle size around a few nanometres. These results reveal that the $\text{Ni}_{0.5}\text{Zn}_{0.5}\text{Fe}_2\text{O}_4$ in the composite films is electrically insulating for $\text{Ni}_{0.5}\text{Zn}_{0.5}\text{Fe}_2\text{O}_4$, thus exhibiting promising magnetic properties for suitable proportions of $\text{Co}_{0.65}\text{Fe}_{0.35}$. They also reveal that the films show in-plane isotropy, in-plane uniaxial anisotropy and super paramagnetic magnetic properties while x changes from 0 to 0.16. In particular, for the samples with $x = 0.085$ and $x = 0.116$, the saturation magnetizations are 1.41 T and 1.19 T, the resistivities reach $677 \mu\Omega \text{ cm}$ and $1371 \mu\Omega \text{ cm}$, the real part of the complex permeability is more than 100 and 150 below 2.0 GHz and the ferromagnetic resonance frequencies reach 3.61 GHz and 2.84 GHz, respectively.

(Some figures in this article are in colour only in the electronic version)

1. Introduction

Soft magnetic films with excellent high frequency characteristics are much required as core materials for use in magnetic components for the ceaseless increase in the working frequency for data transmission and multiple access in computers, mobiles and bluetooth devices [1–6]. The basic requirements for these films are high resistivity ρ , high permeability μ , high saturation magnetization M_s and appropriate anisotropy field H_k . Metal–insulator granular films consisting of magnetic metal nanogranules uniformly distributed in an insulator matrix are among the best candidates for satisfying these demands, because these films have the advantages of good magnetic metal performance with high M_s and high μ and good insulator performance with high ρ . Up to now, soft

magnetic properties of K – M – X films have been reported [1, 7–12], where K is a magnetic metal (Fe, Co, Ni and their alloys), M is a nonmagnetic element (Hf, Mg, Al, Si, Zr, etc) and X is a second period element N, O, F. The mechanism of soft magnetic properties of magnetic granular films has been confirmed to be the exchange coupling between granules through the intergranular regions [13, 14]. As the inserted insulators are nonmagnetic materials, this would result in low M_s for the granular films.

In order to obtain in-plane uniaxial anisotropy magnetic thin films with both high M_s and high ρ , a material with both high resistivity and magnetic properties for the inserted insulator can be selected. With the magnetic adulterant, granular films with high M_s and high ρ may be obtained. Some works on discontinuous metal–native oxide multilayers were studied and high resistivity and high M_s were obtained

¹ Author to whom any correspondence should be addressed.

[15, 16]. As there are no works focused on the properties of granular films with magnetic adulterant systems, NiZn ferrites with electric insulating and soft magnetic properties were used as the adulterant for granular films in this work. The structures, electrical and magnetic properties of these bi-magnetic composite granular films were also studied.

2. Experimental details

The samples were prepared by radio frequency (rf) sputtering onto 10 mm × 20 mm × 0.42 mm (1 1 1)-oriented Si substrates attached to a water-cooling system at room temperature with a background pressure lower than 5×10^{-5} Pa. A Co target, 70 mm in diameter and 3 mm in thickness, on which Fe chips and $\text{Ni}_{0.5}\text{Zn}_{0.5}\text{Fe}_2\text{O}_4$ chips were placed in a regular manner and with the target–substrate distance fixed as 9.0 cm, was used to deposit $(\text{Co}_{0.65}\text{Fe}_{0.35})_{1-x}(\text{Ni}_{0.5}\text{Zn}_{0.5}\text{Fe}_2\text{O}_4)_x$ composite granular films. (Actually, the ratios of Co to Fe are not exactly the same for our samples, but we change the number and size of Fe chips which were placed on the Co target to make sure that the composition of Co and Fe of thin film is almost the same, so we mark all the samples as $(\text{Co}_{0.65}\text{Fe}_{0.35})_{1-x}(\text{Ni}_{0.5}\text{Zn}_{0.5}\text{Fe}_2\text{O}_4)_x$.) The samples were deposited at an angle of 24° with the substrate normal to attain uniaxial anisotropy [17, 18]. The composition of the deposited magnetic layers was adjusted by controlling the numbers and sizes of the Fe chips and $\text{Ni}_{0.5}\text{Zn}_{0.5}\text{Fe}_2\text{O}_4$ chips. During sputtering, an Ar flow rate of 20 sccm (sccm denotes cubic centimetre per minute at STP) was needed to maintain an Ar pressure of 0.15 Pa, and the rf power density was 1.7 W cm^{-2} .

The compositions of the films and the target were measured by energy dispersive x-ray spectroscopy (EDS). The values of x were determined by the ratios of Ni, Zn, Fe and Co of the films which were carried out by EDS results. The crystalline structure was characterized by grazing incidence x-ray diffraction (GIXRD, X'Pert PRO PANalytical with Cu K α radiation). A field emission scanning electron microscope (SEM, Hitachi S-4800) was employed to observe the morphological characteristics of the films. The magnetic hysteresis loops of the films were measured at room temperature using a vibrating sample magnetometer (VSM, Lakeshore 7304 model). The direction of the applied magnetic field was parallel to the film plane. $\mu_0 M_s$ and H_c were obtained from the loops. Permeability spectra were carried out with a PNA E8363B vector network analyzer using the microstrip method from 100 MHz to 8 GHz with the sample (5 mm × 5 mm × 0.42 mm) positioned in the middle of the strip line with an inner height of 0.8 mm between the upper line and the ground plate, the width of the upper line being 3.94 mm and the length being 9 mm [19].

3. Results and discussion

Figures 1 and 2 show the GIXRD and high-resolution scanning electron microscopy (SEM) patterns of the $(\text{Co}_{0.65}\text{Fe}_{0.35})_{1-x}(\text{Ni}_{0.5}\text{Zn}_{0.5}\text{Fe}_2\text{O}_4)_x$ composite granular films with different fractions x of $\text{Ni}_{0.5}\text{Zn}_{0.5}\text{Fe}_2\text{O}_4$. From figure 1, it can be seen that pure $\text{Co}_{0.65}\text{Fe}_{0.35}$ films show a bcc crystal

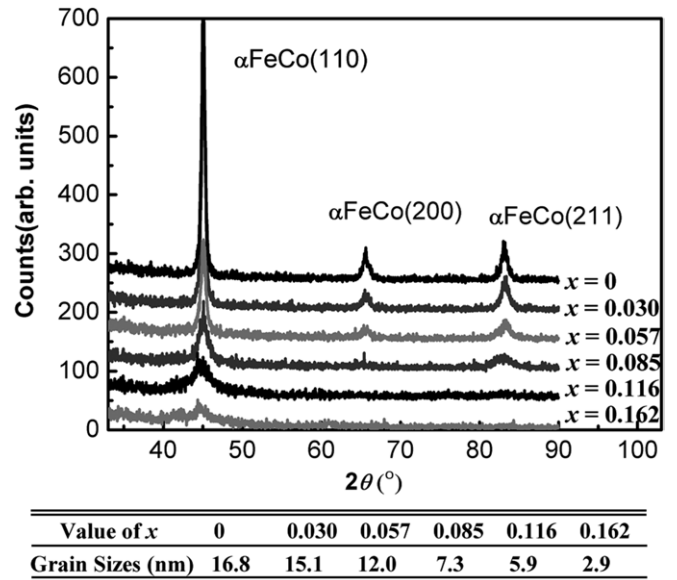


Figure 1. GIXRD spectra of $(\text{Co}_{0.65}\text{Fe}_{0.35})_{1-x}(\text{Ni}_{0.5}\text{Zn}_{0.5}\text{Fe}_2\text{O}_4)_x$ composite granular films with different fractions x . The grain sizes calculated by the Scherrer equation are listed in the table.

lattice structure with the (1 1 0), (2 0 0) and (2 1 1) peaks. With all series, the (1 1 0) peak can be found, but no peaks are related to oxides. This indicates that the ferrites are deposited as amorphous phases, and the bcc structure $\text{Co}_{0.65}\text{Fe}_{0.35}$ is the main phase in the films. It is known that the grain sizes are in inverse proportion to the peak width of XRD by the Scherrer equation [20]. The results are listed in figure 1 as a table. For the $(\text{Co}_{0.65}\text{Fe}_{0.35})_{1-x}(\text{Ni}_{0.5}\text{Zn}_{0.5}\text{Fe}_2\text{O}_4)_x$ composite granular films, the larger the value of x , the smaller the $\text{Co}_{0.65}\text{Fe}_{0.35}$ grain becomes. However, SEM photos show that the particle sizes of $x = 0.030$ are slightly bigger than that of the pure $\text{Co}_{0.65}\text{Fe}_{0.35}$ film. A possible reason is that particles consist of crystalline $\text{Co}_{0.65}\text{Fe}_{0.35}$ grain and amorphous oxide. It is known that during sputtering of the film, the oxygen atoms of NiZn ferrite may escape and combine with $\text{Co}_{0.65}\text{Fe}_{0.35}$ as oxides. The particles in the SEM photos are the composed particles with both $\text{Co}_{0.65}\text{Fe}_{0.35}$ grain and amorphous oxides. The grain sizes calculated by the Scherrer equation are only the $\text{Co}_{0.65}\text{Fe}_{0.35}$ grain sizes.

The SEM photos also reveal that for the samples with $x = 0, 0.030$ and 0.057 , particles show an irregular shape, but for the samples with $x = 0.085, 0.116$ and 0.162 , the photos show continuous films. This result can be explained by the fact that the deposited oxides (including the NiZn ferrite and the oxidized $\text{Co}_{0.65}\text{Fe}_{0.35}$) are amorphous, and the nanograins of $\text{Co}_{0.65}\text{Fe}_{0.35}$ symmetrically fill in the sphere of oxides. The photos show us only the surface of the composed structure, so continuous films are seen in the SEM photos.

The magnetic and electrical properties are based on the peculiar structures discussed in the last part with good magnetic properties of the metal grains and the insulating oxide spheres. Figure 3 shows the saturation magnetization M_s and the resistivities ρ of the samples as a function of x . It can be seen that M_s shows a linear decrease as x increases. It can be easily understood that M_s is equal to the total moment

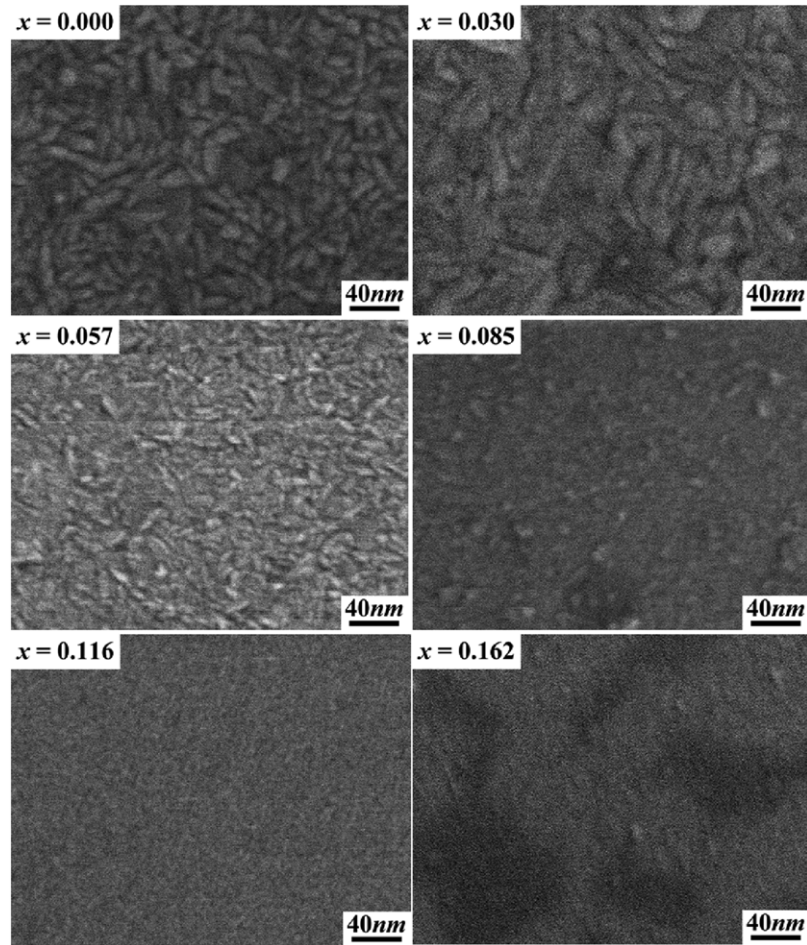


Figure 2. SEM images for $(\text{Co}_{0.65}\text{Fe}_{0.35})_{1-x}(\text{Ni}_{0.5}\text{Zn}_{0.5}\text{Fe}_2\text{O}_4)_x$ composite granular films with different fraction x .

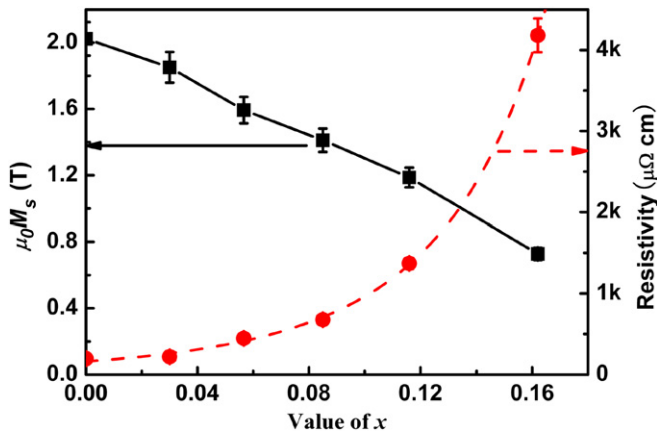


Figure 3. Saturation magnetization $\mu_0 M_s$ and resistivity ρ as a function of component of ferrites for $(\text{Co}_{0.65}\text{Fe}_{0.35})_{1-x}(\text{Ni}_{0.5}\text{Zn}_{0.5}\text{Fe}_2\text{O}_4)_x$ composite granular films.

divided by the volume and then the total moment decreases while the atom fraction x increases. As x is the atom fraction and the molecular weight of ferrite is four times larger than $\text{Co}_{0.65}\text{Fe}_{0.35}$, the volume fraction is larger than the atom fraction. The increase of resistivity (ρ) with increasing x is caused by the presence of more and more insulator content in the films. The relationship of resistivity and x can be fitted by

the percolation formula [21]

$$\rho \propto \rho_0(1 - x - p_c)^{-\alpha}, \quad (1)$$

where ρ_0 is the resistivity of CoFe , p_c is the percolation threshold and α is the critical exponent. The fitting results are also shown in figure 3.

Figure 4 shows the magnetic hysteresis loops of the $(\text{Co}_{0.65}\text{Fe}_{0.35})_{1-x}(\text{Ni}_{0.5}\text{Zn}_{0.5}\text{Fe}_2\text{O}_4)_x$ composite granular films with different fractions. Figure 5 shows the coercivities of the easy axis and the hard axis H_{ce} , H_{cd} and in-plane anisotropy H_k as a function of fraction x . For the samples with $x = 0$ and $x = 0.030$, the magnetic hysteresis loops show no in-plane uniaxial anisotropy and the large coercivities are 2.13 and 2.58 kA m^{-1} , the coercivity of the latter higher than that of the former. The reason is that grain sizes of $\text{Co}_{0.65}\text{Fe}_{0.35}$ are almost the same, but the distance between the metal grains is increased. For $x = 0.057$, the loops show weak in-plane uniaxial anisotropy with $H_k = 3.25 \text{ kA m}^{-1}$, $H_{ce} = 2.42 \text{ kA m}^{-1}$ and $H_{ch} = 0.81 \text{ kA m}^{-1}$, respectively. For this sample of $x = 0.057$, the weak anisotropy is caused by the shape of the grains and the exchange coupling between the neighbouring grains. When the fraction is equal to 0.085 and 0.116, the XRD shows that the grain sizes are very small, and the SEM shows that these films are continuous. The strong exchange coupling between the granules and the small magnetocrystalline anisotropy induce

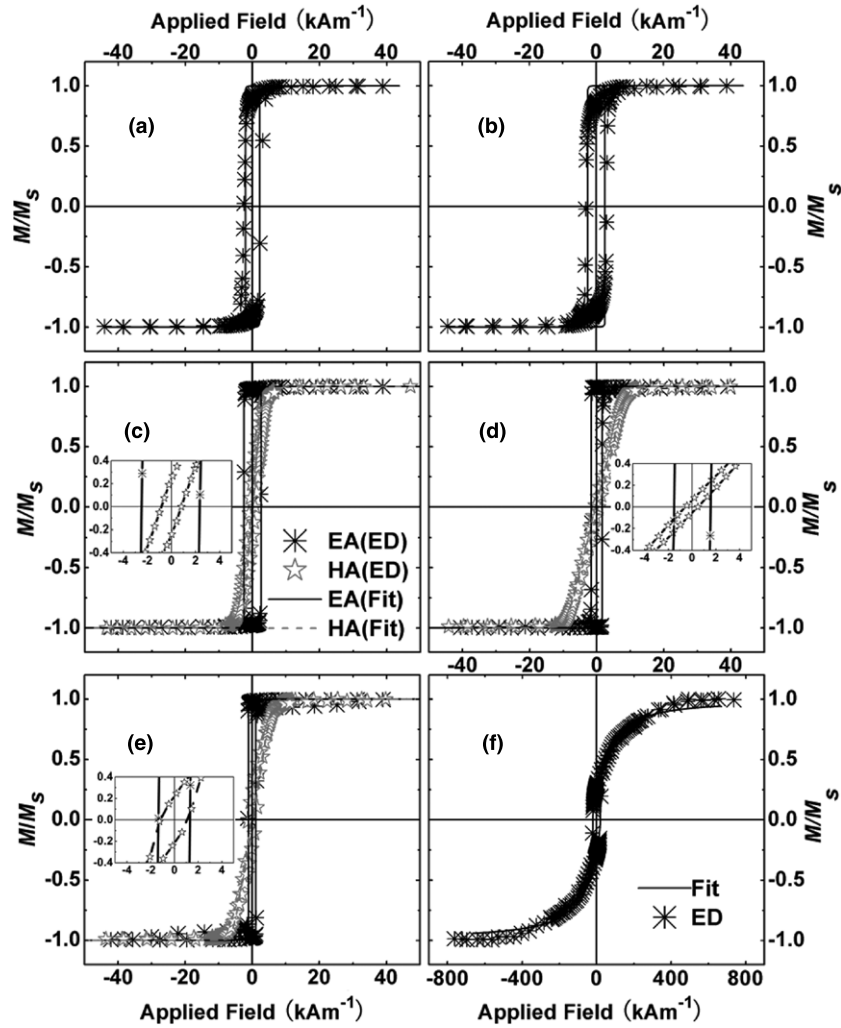


Figure 4. The magnetic hysteresis loops of the $(\text{Co}_{0.65}\text{Fe}_{0.35})_{1-x}(\text{Ni}_{0.5}\text{Zn}_{0.5}\text{Fe}_2\text{O}_4)_x$ composite granular films with different fractions $x = 0.0$ (a), $x = 0.030$ (b), $x = 0.057$ (c), $x = 0.085$ (d), $x = 0.116$ (e), $x = 0.162$ (f). ‘ED’ means experimental data, ‘Fit’ means fitting curves, ‘EA’ means easy axis loops and ‘HA’ means hard axis loops. Samples with no in-plane uniaxial anisotropy are marked with black lines for fitting curves and star points for experimental data.

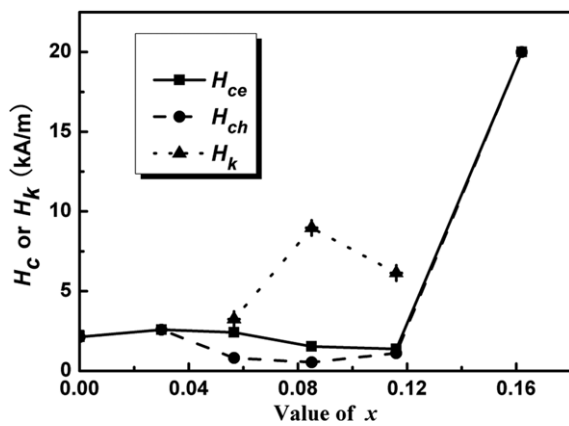


Figure 5. The coercivity of easy axis and hard axis H_{ce} , H_{ch} and in-plane anisotropy field H_k as a function of component of $\text{Ni}_{0.5}\text{Zn}_{0.5}\text{Fe}_2\text{O}_4$.

good soft magnetic properties. For the samples with $x = 0.085$ and 0.116 , $H_k = 8.97 \text{ kA m}^{-1}$ and 6.14 kA m^{-1} , $H_{ce} = 1.53 \text{ kA m}^{-1}$ and 1.38 kA m^{-1} and $H_{ch} = 0.54 \text{ kA m}^{-1}$ and 1.11 kA m^{-1} , respectively. For the sample with $x = 0.162$,

the magnetic hysteresis loop shows a very high coercivity of 20.0 kA m^{-1} . This coercivity has the same quantity as the magnetocrystalline anisotropy field. This means that there are no exchange couple interactions between the granules. A model with superparamagnetic grains is used to fit the experimental data as shown in figure 4(f). Here the Langevin equation is used to describe the superparamagnetic behaviour [22]. The theoretical results are in good agreement with the experimental data. This proves that the granular films with large content of $\text{Ni}_{0.5}\text{Zn}_{0.5}\text{Fe}_2\text{O}_4$ were superparamagnetic-like films.

The magnetic spectra of the samples with in-plane uniaxial anisotropy are shown in figure 6. The spectra were fitted using the theoretical spectra which were determined by the Landau–Lifshitz–Gilbert equation [23]. When x increases, significant changes can be found for the magnetic spectra. This behaviour can be described with the Kittel equation [$f_r = \gamma/2\pi(M_s \cdot H_k)^{1/2}$] for magnetic resonance [24]. With this equation, it is easy to know that the resonance frequency increases when M_s and H_k increase. As $\mu = 1 + M_s/H_k$, the value of the real part of the permeability increases when M_s

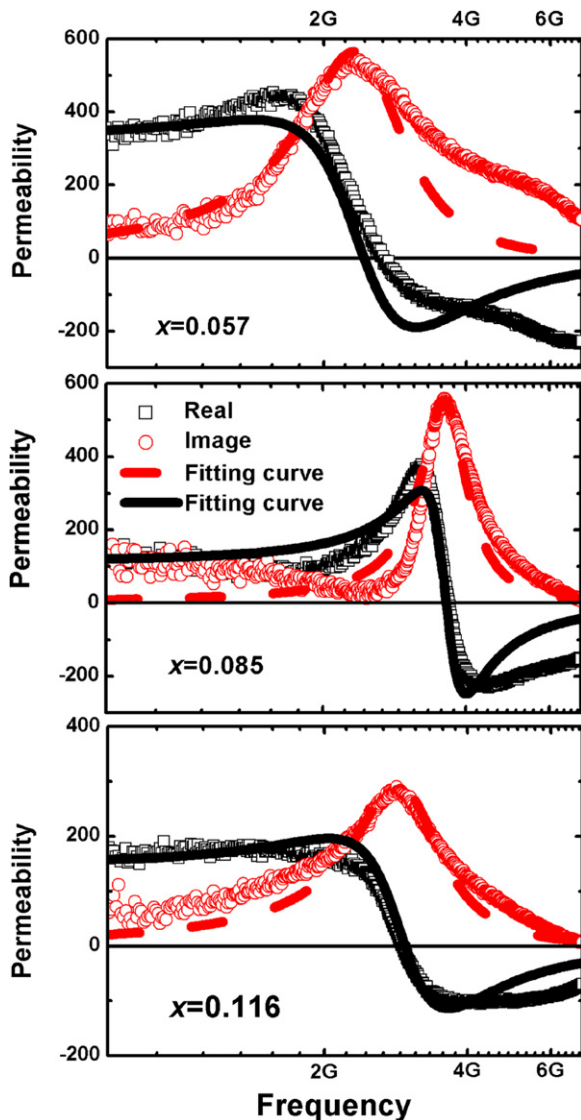


Figure 6. Dependence of complex permeability on frequency for the samples with $x = 0.057, 0.085$ and 0.116 . The black solid lines and red dashed lines show the fitting curves of real parts and imaginary parts of permeability as a function of frequency.

increases, but decreases when H_k increases. For these three samples, the values of M_s are 1.59, 1.41 and 1.19 T, and the values of H_k are 3.25, 8.97 and 6.14 kA m⁻¹. Since the changes in H_k are much larger than those in M_s and the changes in the magnetic spectrum were mainly caused by H_k , the magnetic spectrum of the sample with $x = 0.085$ shows the largest resonance frequency and the lowest permeability.

The shapes of the magnetic spectra also show obvious changes. The second magnetic spectrum shows a sharper shape than the other two spectra. The fact that the shapes of the magnetic spectra are strongly damped by a damping factor is proved elsewhere [25]. By fitting the magnetic spectra with the theoretical spectra, the values of the damping factor were found to be 0.036, 0.025 and 0.044 for $x = 0.057, 0.085$ and 0.116 . These results are in good agreement with the shape changes of the magnetic spectrum.

It can be seen that the real part of permeability is more than 100 and 150 below 2.0 GHz, and the imaginary part gradually

increases to a maximum at $f = 3.61$ GHz and 2.84 GHz for samples with $x = 0.085$ and 0.116 , respectively. The high permeability and resonance frequency imply that the granular films are promising for applications in the high frequency range.

It is worth comparing our results with those of well-known systems. Firstly, for our samples, high saturation magnetizations (1.41 and 1.19 T) and resistivities (677 and 1371 $\mu\Omega$ cm) were obtained for the samples with an in-plane uniaxial anisotropy. For Co–Al–O [8], $\mu_0 M_s = 1.07$ and 1.05 T while $\rho = 583$ and 1165 $\mu\Omega$ cm, and for FeZrO [10], $\mu_0 M_s = 1.3$ T while $\rho = 660$ $\mu\Omega$ cm. Secondly, the $(\text{Co}_{0.65}\text{Fe}_{0.35})_{1-x}(\text{Ni}_{0.5}\text{Zn}_{0.5}\text{Fe}_2\text{O}_4)_x$ composite granular films were prepared by radio frequency magnetron sputtering in a pure Ar gas environment. This method is much easier for controlling the condition of sputtering than the reactive sputtering used for current works.

4. Conclusions

$(\text{Co}_{0.65}\text{Fe}_{0.35})_{1-x}(\text{Ni}_{0.5}\text{Zn}_{0.5}\text{Fe}_2\text{O}_4)_x$ granular films were successfully fabricated by magnetron sputtering and good soft magnetic properties have been obtained with high resistivity and high saturation magnetization. For the typical samples of $x = 0.085$ and $x = 0.116$, the resistivities reach 677 and 1371 $\mu\Omega$ cm and saturation magnetizations are 1.41 and 1.19 T. At frequencies lower than 1.0 GHz, the real parts of the complex relative permeability of these two samples are more than 100 and 150, and the resonance frequencies reach 3.61 and 2.84 GHz, which imply that the films are promising for high frequency applications. The magnetic properties may also be improved if the proportion of Fe:Co is added to a level 65:35 (the highest saturation magnetization that occurs in nature).

Acknowledgments

This work was supported by the NSFC (Grant No 10774062) and the Keygrant Project of the Chinese Ministry of Education (No 309027).

References

- [1] Wang S X, Sun N X, Yamaguchi M and Yabukami S 2000 *Nature* **407** 150
- [2] Zhao Y W, Zhang X K and Xiao J Q 2005 *Adv. Mater.* **17** 915
- [3] Yu S H and Yoshimura M 2002 *Adv. Funct. Mater.* **12** 9
- [4] Naito Y and Suetaki K 1971 *IEEE Trans. Microwave Theory Technol.* **19** 65
- [5] Musal H M and Hahn H T 1989 *IEEE Trans. Magn.* **25** 3851
- [6] Chai G Z, Xue D S, Fan X L, Li X L and Guo D W 2008 *Appl. Phys. Lett.* **93** 152516
- [7] Morikawa T, Suzuki M and Taga Y 1998 *J. Appl. Phys.* **83** 6664
- [8] Ohnuma M, Hono K, Onodera H, Ohnuma S, Fujimori H and Pedersen J S 2000 *J. Appl. Phys.* **87** 817
- [9] Ohnuma S, Lee H J, Kobayashi N, Fujimori H and Masumoto T 2001 *IEEE Trans. Magn.* **37** 2251
- [10] Hayakawa Y, Makino A, Fujimori H and Inoue A 1997 *J. Appl. Phys.* **81** 3747

- [11] Ohnuma S, Fujimori H, Mitani S and Masumoto T 1996 *J. Appl. Phys.* **79** 5130
- [12] Yao D S, Ge S H, Zhang B M, Zuo H P and Zhou X Y 2008 *J. Appl. Phys.* **103** 113901
- [13] Herzer G 1990 *IEEE Trans. Magn.* **26** 1397
- [14] Xue D S, Chai G Z, Li X L and Fan X L 2008 *J. Magn. Magn. Mater.* **320** 1541
- [15] Beach G S D, Berkowitz A E, Parker F T and Smith D J 2001 *Appl. Phys. Lett.* **79** 224
- [16] Jurca I S, Meny C, Viart N, Ulhaq-Bouillet C, Panissod P and Pourroy G 2003 *Thin Solid Films* **444** 58
- [17] Fan X L, Xue D S, Lin M, Zhang Z M, Guo D W, Jiang C J and Wei J Q 2008 *Appl. Phys. Lett.* **92** 222505
- [18] Li W D, Kitakami O and Shimada Y 1998 *J. Appl. Phys.* **83** 6661
- [19] Bekker V, Seemann K and Leiste H 2004 *J. Magn. Magn. Mater.* **270** 327
- [20] Patterson A L 1939 *Phys. Rev.* **56** 978
- [21] Rosenbaum T F, Andres K, Thomas G A and Bhatt R N 1980 *Phys. Rev. Lett.* **45** 1723
- [22] Franco V, Conde C F, Conde A and Kiss L F 2005 *Phys. Rev. B* **72** 174424
- [23] Gilbert T L 2004 *IEEE Trans. Magn.* **40** 3443
- [24] Kittel C 1948 *Phys. Rev.* **73** 155
- [25] Liu Y, Tan C Y, Liu Z W and Ong C K 2007 *J. Appl. Phys.* **101** 023912